FINITE ELEMENT MODELING OF THE ARCHING EFFECT IN RETAINING WALLS MADE OF SOIL-CEMENT COLUMNS

Nicolas Denies, Belgian Building Research Institute, Geotechnical Division, Belgium, nde@bbri.be
Malek Allani, Belgian Building Research Institute, BBRI, Limelette, Belgium, mal@bbri.be
Noël Huybrechts, Belgian Building Research Institute & KU Leuven, Belgium, nh@bbri.be
Jean-Cédric Kouamé, Franki Foundations Belgium SA, Saintes, Belgium, Jean-Cedric.Kouame@ffgb.be
Grégory Laurent, Franki Foundations Belgium SA, Saintes, Belgium, Gregory.Laurent@ffgb.be
Tim Eggermont, Franki Foundations Belgium SA, Saintes, Belgium, Tim.Eggermont@ffgb.be
Maurice Bottiau, Franki Foundations Belgium SA, Saintes, Belgium, mail@ffgb.be

ABSTRACT

Deep Mixing is increasingly applied for the construction of retaining structures. The working principle of a soil mix wall with a retaining function is mainly based on the development of an arching effect through the soil mix material to transmit the earth and water pressures, acting behind the retaining wall, to the steel beams inserted in the fresh soil mix material during execution. Example calculations of the arching effect in Plaxis 2D have recently been provided for rectangular panels in the BBRI/SBRCURnet Handbook - Soil mix walls, referred as the handbook in the present paper. Nevertheless, there is a lack of information regarding the transmission of the forces inside a wall made of soil-cement columns. The present paper describes finite element models of this kind of wall, implemented to illustrate the way the forces are internally transmitted, considering the ground anchors ensuring the horizontal stability of the wall and the steel beams ensuring its bending resistance. A comparison is also made between numerical results of a model, at a depth without ground anchor, and the analytical solutions proposed in the handbook for the verification of the soil mix walls in agreement with the Eurocodes. If the results are comparable, a significant difference is still observed for the maximal compressive stress computed in the middle of the pressure arch.

Keywords: soil mix walls, retaining walls, soil-cement columns, FEM, arching effect, design

INTRODUCTION – RETAINING WALL MADE OF SOIL-CEMENT COLUMNS AND FEM OF THE TRANSMISSION OF THE FORCES INSIDE THE WALL

In order to build a retaining wall for the realization of an excavation, soil-cement columns can be placed next to each other, in a secant way (see Fig. 1). The diameter of these columns often ranges between 0.4 to 0.6 m and they present installation depths up to 20 m. By overlapping the soil-cement columns, a continuous retaining wall is built. The wall is then horizontally stabilized with the help of bracing or anchoring systems. During execution, steel H or I-beams are generally installed in the fresh soil mix material to resist the shear forces and bending moments due to the pressure applying on the wall. The soil mix material mainly transmits the stresses due to this pressure to the steel beams by way of an arching effect developing in the soil mix due to the difference of stiffness between the steel and the soil mix material. Figure 1 illustrates the working principle of a soil mix wall with a retaining function. This picture is given for a rectangular panel as this geometry has intensively been studied in a recent past. The present paper analyzes the transmission of the forces inside a wall made of soil-cement columns. For that purpose, two types of FEM models, built with PLAXIS 2D, are used. A first type of model investigates the transfer of the forces in the wall at the depth presenting ground anchors. A second type of model highlights the development of the arching effect between the steel beams. A comparison is made between the results of the second model and the analytical solutions given in the handbook. In both kinds of models, a uniform pressure of 50 kPa (corresponding depth of about 5 m) is applied on the soil mix material which is modeled with an elasto-plastic behavior and a failure criterion type Mohr-Coulomb. We are working in plane strain configuration (no vertical deformation). The soil mix material can freely move in the direction of the pressure load, but the deformations and displacements are prevented in the lateral directions, at the model boundaries.

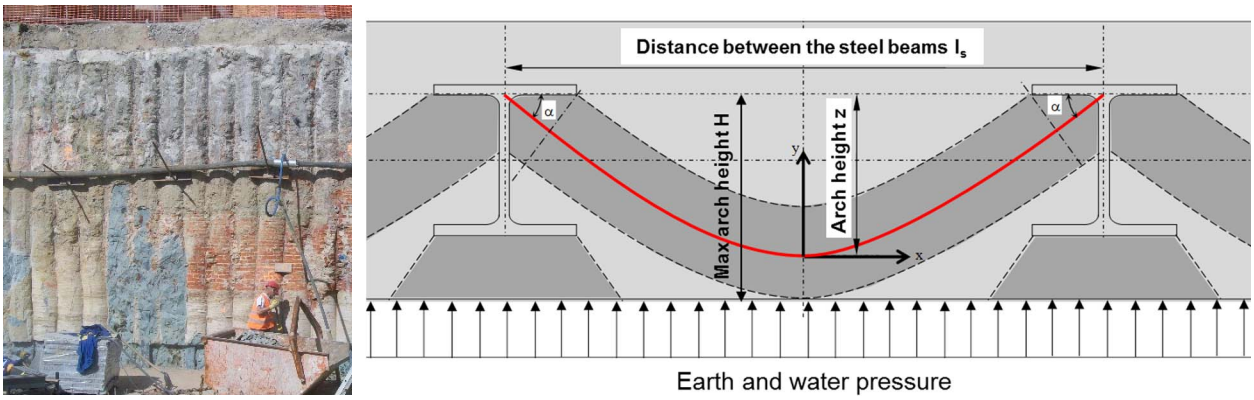

Fig. 1. Working principle of a soil mix retaining wall and illustration of the arching effect

TRANSMISSION OF THE FORCES IN THE SOIL MIX BETWEEN THE GROUND ANCHORS

In the first model (see Fig. 2), the displacement of the ground anchors is prevented with fixed points, called fixed-end anchors in Plaxis, commonly used in FEM's to simulate ground anchors supporting retaining walls. Table 1 presents the data of the model. For the initial simulations, a coarse mesh is used without local refinement. The axis-to-axis distance between the ground anchors is set to 2.08 m (i.e. every four columns). Rigid interface elements presenting the same strength than the soil mix material are used around the steel beams and the ground anchors. The soil surrounding the columns is modeled with the hardening soil model with small strain stiffness and it is only used to transmit the earth-water pressure to the columns.

For the first series of simulations, the dimensions and the mechanical properties of the anchor plates are randomly taken as those of the flange of the IPE 270. Figure 3 illustrates the development of the principal total stress σ_1 in the soil mix wall. Once the stress concentrations around the **anchor plates** are eliminated, pressure arches are observed in the soil mix material developing between the ground anchors. In the next simulations, anchor plates with dimensions and properties representative of the geotechnical practice will be used to analyze their influence. With the three pressure arches modeled in the simulations, **boundaries effects** are highlighted based on the maximal value of the total normal stresses developing in the middle of each pressure arch (difference of 18% between the value of the central arch, σ_N = 863 kPa, and the values of the two others). The asymmetry in terms of total normal stress in the left (σ_N = 1037 kPa) and the right (σ_N = 1059 kPa) arches is about 2%.

In the second series of simulations, anchor plates as commonly used on the field are used (thickness 2 cm, height and width 30 cm). The boundary effects are studied considering four models with 1, 3, 5 and 7 pressures arches simulated in FEM's with $f_{sm,tk}$ = 0.4 MPa. Table 2 compares the total normal stresses developing in the middle of the central arch. As a result, the model simulating five pressure arches seems to be a good compromise regarding the boundary effects. With smaller models, the stresses developing in the soil mix material could be overestimated. Conclusion is the same for the anchor plate, the use of anchor plates representative for those used on the field decreases the stress in the soil mix material.

Influence of the **mesh refinement** is also regarded. With a fine mesh, singular points with important stress concentration emerge in the soil mix wall at the interface between the secant columns. In order to avoid these numerical singularities resulting in an overestimation of the stress in the soil mix material, an adapted geometry of the wall was established (see Fig. 4). With that adaptation, similar stress values were obtained with the models independently of the mesh refinement, as illustrated by the two last lines of values in Table 2. Figure 5 illustrates the principal total stress σ_1 in the central arch of the soil mix wall obtained with the finite element model including 5 arches, representative anchor plates and an adapted geometry. This model will be referred as the "reference model" in the following.

Table 1. Data, geometry and parameters of the present model

Soil mix parameters	
Diameter of the soil-cement column, d_1	0.6 m
Characteristic value of the Unconfined Compressive Strength (UCS) of the soil mix material, $f_{sm,k}$	4.0 MPa
Modulus of elasticity, E_{sm} (with E_{sm} = 1000 $f_{sm,k}$ in first approximation as referred in the handbook)	4.0 GPa
Charcteristic value of the tensile strength of the soil mix material, $f_{sm,tk}$	variable
Cohesion of the soil mix material, c'	2000 kPa
Internal friction angle of the soil mix material, ϕ'	0.1°
Steel beam parameters	
Type of steel beam	IPE 270
Modulus of elasticity of the steel	210 GPa
Height of the beam, h_a	270 mm
Thickness of the web, t_w	6.6 mm
Width of the flange, b_f	135 mm
Thickness of the flange, t_f	10.2 mm
Axis-to-axis distance between the steel beams, l_s	1.04 m
Beam covers considering an equivalent height for the wall (compressive and tensile sides): $c_1 = c_2$	121 mm

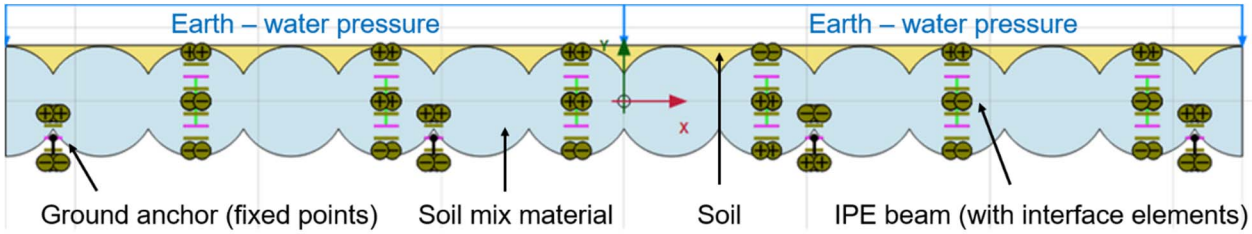

Fig. 2. First type of FEM used to simulate a soil mix wall made of soil-cement columns

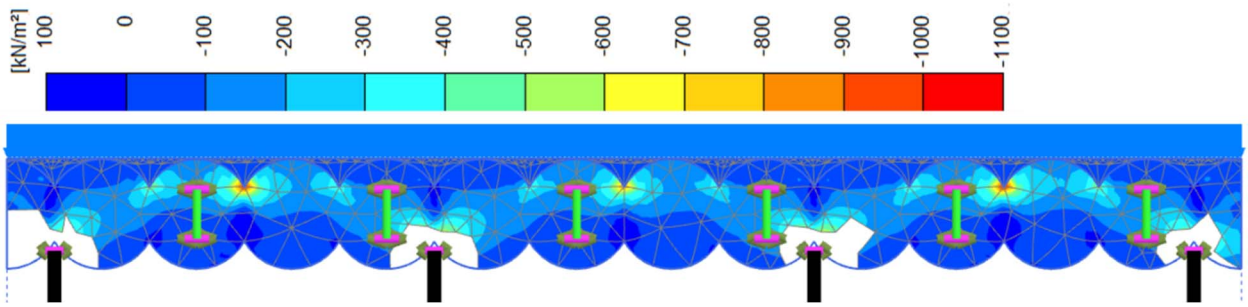

Fig. 3. Principal total stress σ_1 in the soil mix wall after elimination of the stress concentration around the ground anchors (simulations with three modeled pressure arches and $f_{sm,tk}$ = 0.2 MPa)

In conclusion, FEM with five modeled arches seems to be a good compromise to simulate the stress distribution in a wall made of soil-cement columns but an adapted geometry must be considered to provide a model independent of the mesh refinement. In addition, a special attention must be brought to the anchor plates whose dimensions and properties must be representative of the reality. Indeed, if no global failure of the wall is observed with an applied pressure of 50 kPa (or 100 kPa), plastic points, where the tensile strength of the soil mix material is reached, are still observed in the axis of the ground anchors and the increase of the applied pressure will accentuate this phenomenon (see Fig. 6). Considering the emergence of these plastic points in the axis of the ground anchors, the punching failure mode (arising behind the anchor seat) should be regarded with caution. A solution for the verification of the resistance of the soil mix material against punching failure is given in the handbook (see §6.8.10). Plastic points are also observed in the center of the pressure arch. This is probably because the center of the pressure arch develops, in the present geometry, in the most reduced cross-section, i.e. at the interface between the columns.

As a final step of the design process, normal and shear stresses obtained with the "reference model" will be compared with the admissible values of the normal and shear stresses in the soil mix material.

Table 2. Total normal stress in the middle of the central arch for different FEM's ($f_{sm,tk}$ = 0.4 MPa)

Mesh	Finite element model used for the simulations (below) and number of modeled pressure arches (right)	1	3	5	7
Coarse mesh	Total normal stress in the middle of the central arch with anchor plates = flange of the steel beam IPE 270 [kPa]	1422	685	646	649
	Total normal stress in the middle of the central arch with representative anchor plates as used in the practice [kPa]	1406	612	570	558
Fine Mesh	Total normal stress in the middle of the central arch with representative anchor plates as used in the practice [kPa] - without adaptation of the geometry of the soil mix wall	2933	1718	1514	1552
	Total normal stress in the middle of the central arch with representative anchor plates as used in the practice [kPa] - with adaptation of the geometry of the column intersection	902	640	691	700
Coarse mesh	Total normal stress in the middle of the central arch with representative anchor plates as used in the practice [kPa] - with adaptation of the geometry of the column intersection	930	647	**685**	688

Blue arrows in the Table means quasi equivalent

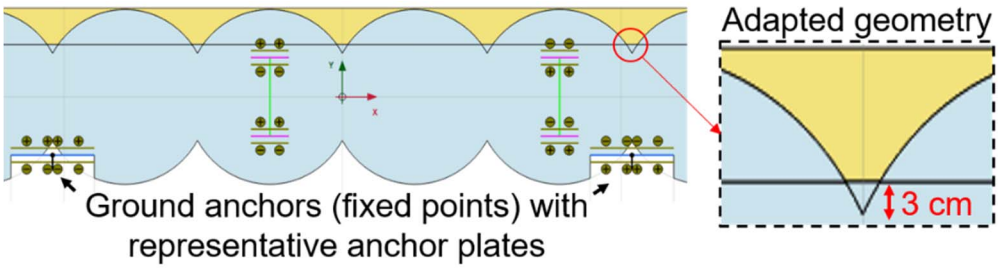

Fig. 4. Adapted geometry of the soil mix wall at the column intersection to avoid singular points

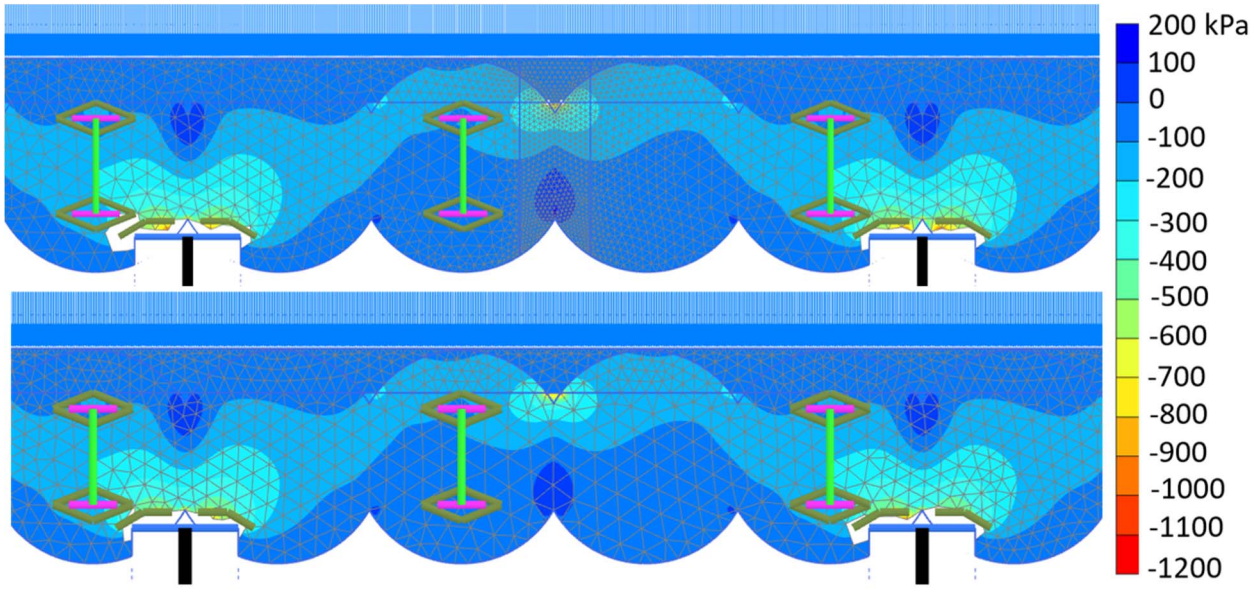

Fig. 5. Principal total stress σ_1 in the soil mix wall after elimination of the stress concentrations around the ground anchors (with $f_{sm,tk}$ = 0.4 MPa). Above: fine mesh, below: coarse mesh

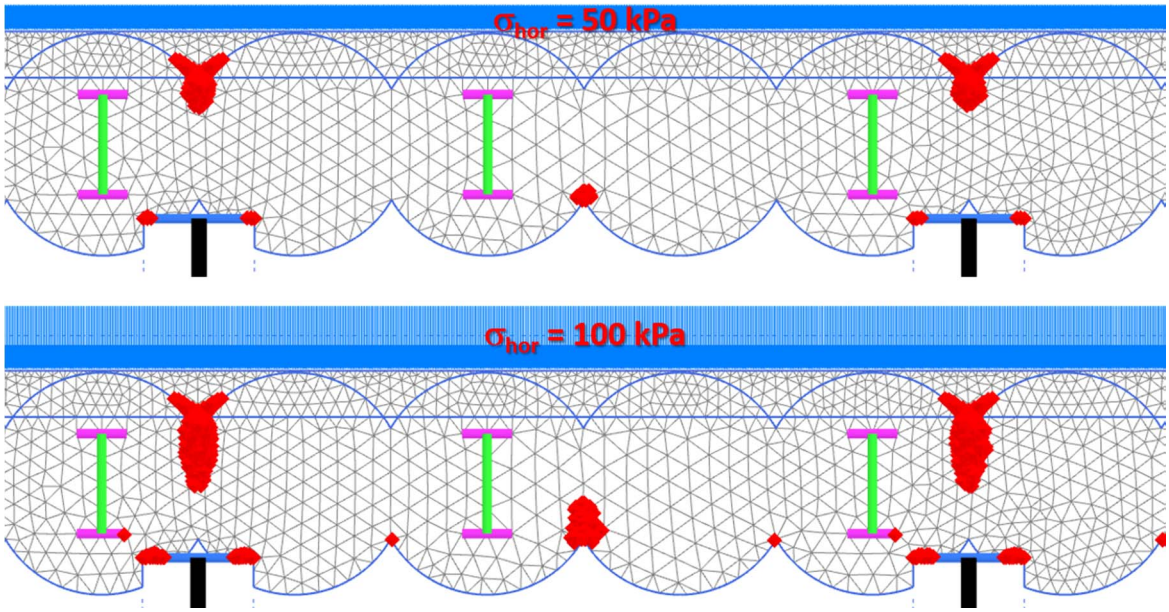

Fig. 6. Development of plastic points (rhombuses) where the tensile resistance of the soil mix material is reached. Above: σ_{hor} = 50 kPa; below: σ_{hor} = 100 kPa (simulations with $f_{sm,tk}$ = 0.4 MPa)

FEM OF THE ARCHING EFFECT DEVELOPING BETWEEN THE STEEL BEAMS

After the study of the transmission of the forces at the level of the ground anchors, the next FEM will highlight the arching effect developing in the soil mix material to transmit the earth-water pressure to the steel beams at a depth without ground anchor. Figure 7 illustrates the pressure arch developing, between the steel beams, in the soil mix material. Data of the model are those of the first simulations (cf. Table 1). The displacement of the steel beams is prevented with fixed points (black anchor lines in Fig. 7). A medium mesh is this time used. Figures 8, 9 and 10 illustrate the stress distributions along selected cross-sections in the soil mix material, respectively: the total normal stresses developing at the base and in the center of the pressure arch and the shear stress developing at a distance $l_s/4$ from the center of the arch.
In order to investigate the **influence of the lateral boundaries**, an extended model with three simulated pressure arches has been implemented. As the stress values, considered along similar cross-sections than for the "one arch" model, are the same in the three pressure arches, there is no boundary effect and the development of the stresses in the pressure arch can be studied with a model simulating one pressure arch.
To study the **effect of the mesh refinement** on the results, a fine mesh is used. Moreover, in areas where large stress concentration or large deformation gradients are expected, local refinements (mesh density multiplied by 5) are applied. The densification and the local refinement of the mesh do not lead to different compressive and shear stress values than those obtained with the medium mesh. The medium mesh is thus suitable for such numerical analysis.

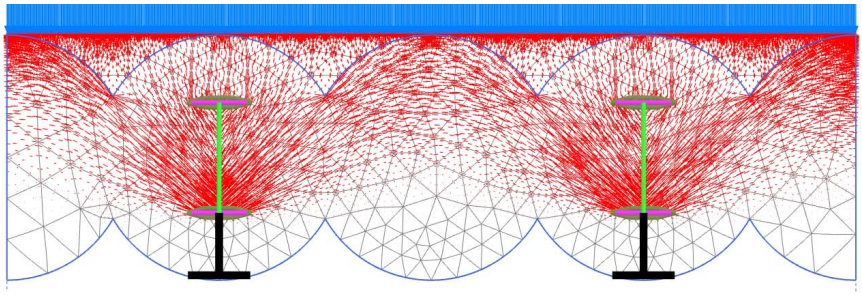

Fig. 7. Development of the arching effect in the soil mix material: effective principal stresses (simulation with $f_{sm,tk}$ = 0 MPa)

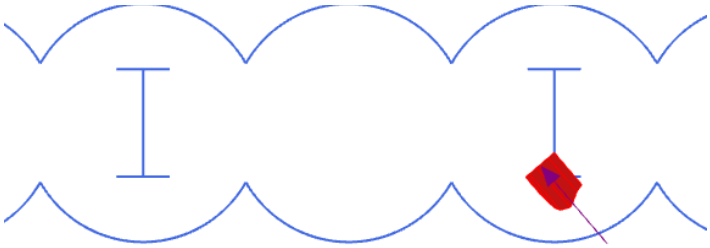

Fig. 8. Total normal stress distribution, σ_N, at the base of the pressure arch (for $f_{sm,tk}$ = 0 MPa)

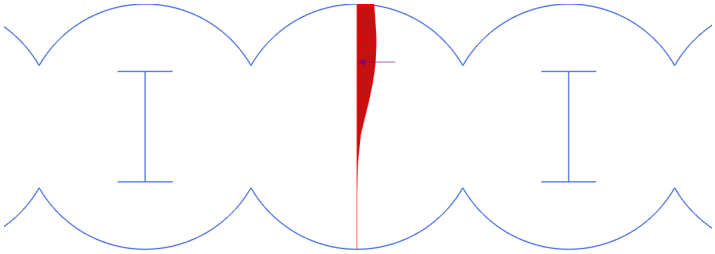

Fig. 9. Total normal stress distribution, σ_N, in the middle of the pressure arch (for $f_{sm,tk}$ = 0 MPa)

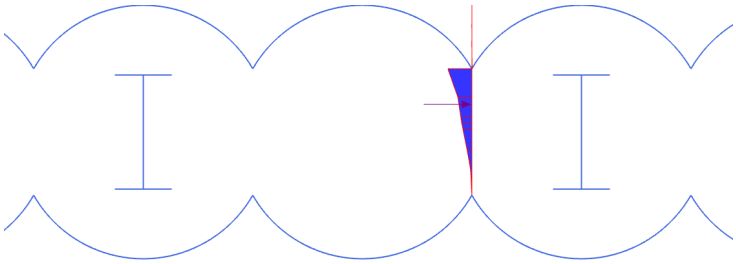

Fig. 10. Shear stress distribution, τ_S, developing along the cross-section at a distance $l_s/4$ from the center of the pressure arch (for $f_{sm,tk}$ = 0 MPa)

VERIFICATION OF THE ARCHING EFFECT ACCORDING TO THE HANDBOOK

In practice, the geotechnical engineer responsible of the design of the soil mix wall generally uses analytical methods, as proposed in the handbook, to check the arching effect (see Fig. 1) according to the Eurocodes. In the present case, a temporary wall made of columns and reinforced with IPE 270 is considered with the properties given in Table 1. Temporary means that the lifetime of the wall is less than 2 years.
The method of the handbook, originally developed for rectangular panels, considers the soil mix wall made of columns as a rectangular panel assuming an equivalent height for the wall. Figure 11 provides the geometrical data for a wall made of soil-cement columns.

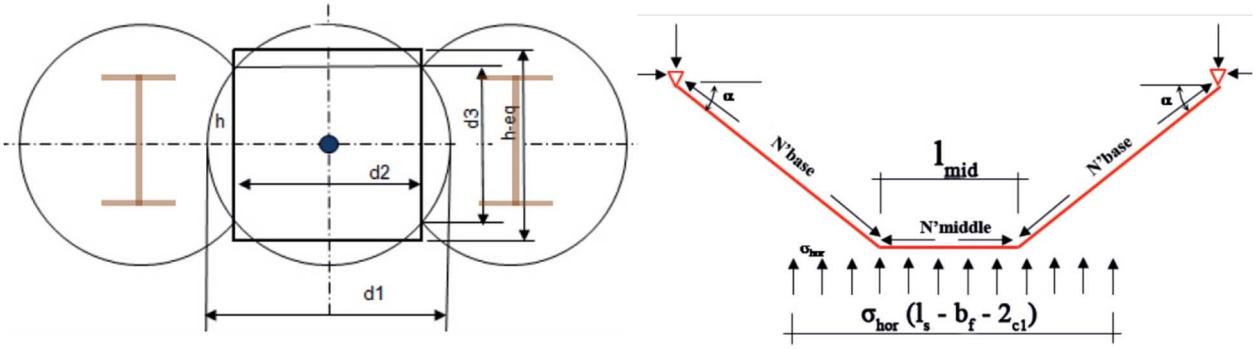

Fig. 11. Geometrical data for a soil mix wall made of columns (left) and "strut and tie" model for the verification of the arching effect according to Eurocode 2 (right)

Considering these definitions, the contact surface width (overlap between columns) and the half thickness of the overlap are respectively defined as:

$$d_3 = \sqrt{d_1^2 - d_2^2} = \sqrt{600^2 - 520^2 =} \; 299.3 \text{ [mm]} \quad [1]$$

$$h = \frac{(d_1 - d_2)}{2} = 40 \text{ [mm]} \quad [2]$$

where $d_2 = 0.5\ l_s = 520$ [mm] with l_s defined in Fig. 1 and Table 1. The net secant column area A_1 will be assessed as:

$$A_1 = \frac{\pi d_1^2}{4} - 2\left[\frac{h}{6d_3}(3h^2 + 4d_3^2)\right] = 266565 \text{ [mm²]} \quad [3]$$

The **equivalent height of the wall** made of soil-cement columns is $h_{sm,eq} = A_1/d_2 = 512.6$ [mm].

Before the verification of the pressure arch, it is still necessary to **determine the UCS design value** of the soil mix material, noted $f_{sm,d}$. According to the definitions of the handbook, $f_{sm,d}$, is determined as:

$$f_{sm,d} = \alpha_{sm} \frac{f_{sm,k}}{\gamma_{sm} k_f} \beta \quad [4]$$

where, α_{sm}, the long-term factor is equal to 1 [-] for temporary and 0.85 [-] for permanent walls. γ_{sm} is the material factor equal to 1.5 in Belgium. k_f is a factor taking into account the way the UCS is determined: if the UCS is determined based on samples from the in situ walls, k_f is equal to 1.0 [-]; in all other cases, e.g. starting from 'estimated' values, this factor is equal to 1.1 [-]. β is a correction factor [-] for the young age of the soil mix material; depending on various factors, $\beta = 0.3$ to 0.7 after 7 hardening days and $\beta = 0.6$ to 0.8 after 14 hardening days. β is used in case of excavation a few days after the execution of the soil mix. In the present case, we consider the following values for these parameters: $\alpha_{sm} = \beta = 1$ [-], $\gamma_{sm} = 1.5$ [-] and $k_f = 1.1$ [-]. In the present case, $f_{sm,d}$ is therefore equal to 2.42 [MPa].

Considering the analytical methods proposed in the handbook, it must be first verified that the earth and water pressures can be transmitted to the steel beams via a pressure arch. According to Eurocode 2, EC2 (EN 1992-1-1), to ensure the arching effect, the **distance between the steel beams** must be limited:

$$l_s < 3H \quad [5]$$

where l_s is the axis-to-axis distance between the steel beams and H the maximal height available for the development of the arch in the soil mix material (see Fig. 1). $H = h_a - t_f + \min(c_1;c_2) = 381$ [mm] where $c_1 = c_2 = (h_{sm,eq} - h_a)/2 = 121$ [mm]. Considering the data of Table 1, that results in: 1.040 [m] < 1.143 [m]. The arching effect is thus verified according to EC 2.

After this first verification, the **geometry of the pressure arch** is broached with the determination of:
- the height of the pressure arch (noted z in Fig. 1),
- the angle α at the location of the base of the pressure arch (illustrated in Fig. 1),
- the thickness of the pressure arch at location of the beam, d_{bg}, and in the middle of the arch, $d_{bg;mid}$.

This determination is made by means of an iterative calculation varying α by assuming a parabolic function for the central line of the arch, i.e. the red line in Fig. 1.
The height of the arch is determined in agreement with the Dutch National Annex of EC2:

$$z_{bg} = 0.2\ l_s + 0.4\ H \leq 0.6\ l_s \quad [6]$$

Moreover, for geometrical reasons:

$$z_{bg} \leq H - \frac{d_{bg;mid}}{3} \quad [7]$$

where $d_{bg;mid}$ is the thickness of the pressure arch in the middle of the arch (cross-section) which is approximated by: $d_{bg;mid} = b_f \tan \alpha$ based on numerical analysis of the development of the pressure arch in the soil mix material. The factor 3 in equation [7] results from the apparent quasi-linear course of the compressive stress in the middle cross-section (see Fig. 9 for the sake of illustration). In the present case, varying α, the verification is finally obtained for the following values: $\alpha = 51.3°$, $d_{bg;mid} = 169$ [mm], $z_{bg} = 325$ [mm]. In addition, the thickness of the pressure arch at the location of the beam can be assessed based on the angle α and considering the flange width of the beam, b_f: $d_{bg} = b_f \sin \alpha = 105$ [mm].

The next stage is the **computation of the stresses developing in the soil mix arch**. This verification is based on a 'strut and tie' model given in Fig. 11.

The maximum compressive stress at the connection with the beam is first regarded. As demonstrated in the FEM calculations, the stress distribution at the location of the base of the beam is equally divided (see Fig. 8 for the sake of illustration). Therefore, the maximum compressive stress can be determined based on a calculated normal force (N'_{base}) and the established thickness of the arch (d_{bg}). A part of the pressure applying on the wall is directly absorbed by the outer flange of the steel beam. The remaining part between the beams is transferred via the pressure arch. If one assumes that loads below 45º can be transferred to the outer flange, the design value (in Ultimate Limit States - ULS) of the load borne by the pressure arch is:

$$F_{hor;pressure\ arch} = F_{hor;tot} - F_{hor;outer\ flange} = \sigma_{hor}\left(l_s - b_f - 2c_1\right) = 33.15 \text{ [N/mm]} \quad [8]$$

with σ_{hor} the design value of the earth and water pressure (σ_{hor} is equal to 50 kPa in the present case study).

Considering the value of the angle α between the pressure arch and a flange beam (51.3°), the occurring normal force at the base of the flange is:

$$N'_{base} = \frac{0.5\, F_{hor;pressure\ arch}}{\sin \alpha} = \frac{0.5\, \sigma_{hor}\left(l_s - b_f - 2c_1\right)}{\sin \alpha} = 21.2 \text{ [N/mm]} \quad [9]$$

As a result, the compressive stress developing in the pressure arch is equal to:

$$\sigma'_{arch,base} = \frac{N'_{base}}{d_{bg}} = \frac{0.5\, \sigma_{hor}\left(l_s - b_f - 2c_1\right)}{\left(b_f \sin^2 \alpha\right)} = 0.201 \text{ [MPa]} \quad [10]$$

The width of the horizontal beam of the strut and tie model of the Fig. 11 is noted l_{mid} and is computed as:

$$l_{mid} = l_s - 2\frac{z_{bg}}{\tan \alpha} = l_s - 2\frac{z_{bg}}{\left(\frac{4 z_{bg}}{l_s}\right)} = \frac{1}{2}\, l_s = 0.52 \text{ [m]} \quad [11]$$

The maximum shear force in the pressure arch is found at the bend in the strut and tie model (see Fig. 11):

$$V_{mid} = 0.5\, l_{mid} \sigma_{hor} = 0.25\, l_s \sigma_{hor} = 12.99 \text{ [N/mm]} \quad [12]$$

Despite the shear stress distribution observed in soil mix wall (see Fig. 10), according to the assumption of the handbook, the design value of the maximum shear stress will be considered parabolic and given by:

$$\tau_{Ed} = \frac{3}{2}\frac{V_{mid}}{d_{bg;mid}} = 0.115 \text{ [MPa]} \quad [13]$$

Finally, the maximum compressive stress in the center of the pressure arch is regarded. Contrarily to the base of the arch, FEM results show that a substantially linear stress distribution is formed in the center (cross-section) of the pressure arch (see Fig. 9). This is calculated on the assumption that the soil mix material cannot absorb any tension. Considering the geometry of the pressure arch in the strut and tie model and the Pythagorean theorem, the resultant normal force in the horizontal beam, N'_{middle}, is given by:

$$N'_{middle} = \sqrt{N'^2_{base} - V^2_{mid}} = 16.7 \text{ [N/mm]} \quad [14]$$

The average compressive stress in the middle of the arch $\sigma'_{arch;mid;avg}$ is then computed as $N'_{middle}/d_{bg;mid} = 0.099$ [MPa]. Nevertheless, the stress in the middle of the arch is not uniform. Assuming that the maximum absorbable tensile stress is reached (which is set equal to 0), on the tensile side, the normal compressive stress resulting of N'_{middle} is completely counterbalanced by the moment. At the compressive side, the compressive stress is then doubled:

$$\sigma'_{arch;mid;max} = 2\,\sigma'_{arch;mid;avg} = 0.198 \text{ [MPa]} \quad [15]$$

Once the compressive and shear stresses arising in the pressure arch are determined, these values must be compared with the **admissible stresses** computed taking into account the resistance of the soil mix material. Distinction is made between the admissible compressive stress in the middle cross-section of the arch (considered as a compressive strut with transverse tension) and the admissible compressive stress at the base of the arch (considered as a connecting node). In the compressive strut, based on the condition that there is a compressive beam with tensile stress in the opposite direction, the design value of the admissible compressive stress in the center of the pressure arch is determined, according to EC2, by:

$$\sigma_{Rd,max,strut} = 0.6\,\nu'\,f_{sm,d} = 0.6\left(1 - \frac{f_{sm,k}}{250}\right)f_{sm,d} = 1.431 \text{ [MPa]} \quad [16]$$

For the connection node, tensile stresses may occur in the vertical direction if the flange of the beam lies within the tensile zone. In consequence, according to EC2, the design value of the admissible compressive stresses at the node is given by:

$$\sigma_{Rd,max,node} = k_2\,\nu' f_{sm,d} = 0.85\left(1 - \frac{f_{sm,k}}{250}\right)f_{sm,d} = 2.028 \text{ [MPa]} \quad [17]$$

The admissible shear stress in the pressure arch is equal to the design value of the shear strength $\tau_{Rsm,d}$ which can be increased by 15% of the compressive stress in the pressure arch:

$$\tau_{Rsm,d} = f_{sm,td} + \frac{15}{100}\sigma'_{arch,mid,av} = \alpha_{sm}\frac{0.21 f^{2/3}_{sm,k}}{\gamma_{sm} k_f}\beta + \frac{15}{100}\sigma'_{arch,mid,av} = 0.336 \text{ [MPa]} \quad [18]$$

where $f_{sm,td}$ is the design value of the tensile strength of the soil mix material. According to EC2, in order to increase the shear strength with a proportion of the compressive stress developing in the pressure arch, $\sigma'_{arch,mid,av}$ (0.099 MPa) must be smaller than 0.2 $f_{sm,d}$ (0.485 MPa).

In the present case, the verification of the internal stresses arising in the pressure arch is established:
$\sigma'_{arch,base} = 0.201$ [MPa] (equation 10) < $\sigma_{Rd,max,node} = 2.028$ [MPa] (equation 17)
$\sigma'_{arch;mid;max} = 0.198$ [MPa] (equation 15) < $\sigma_{Rd,max,strut} = 1.431$ [MPa] (equation 16)
$\tau_{Ed} = 0.115$ [MPa] (equation 13) < $\tau_{Rsm,d} = 0.336$ [MPa] (equation 18)

COMPARISON OF THE FEM RESULTS WITH THE ANALYTICAL RESULTS OF THE HANDBOOK METHODOLOGY FOR THE VERIFICATION OF THE PRESSURE ARCH

In the present case, the finite element model with one arch is used for the comparison which is made considering two tensile strengths for the soil mix material in the simulations: 0.4 and 0 MPa. It is to note that the value of the tensile strength of the soil mix material is not directly used in the analytical verification. The value of the tensile strength introduced in equation [18] is determined based on the characteristic UCS value of the soil mix material, $f_{sm,k}$. Table 3 provides the comparison between the FEM and the analytical results for the compressive and shear stresses arising in the pressure arch resulting from the application of a uniform pressure of 50 kPa on the wall. For the computation of the maximal stresses, cross-sections are selected in the numerical models in such a way that they correspond to the cross-sections considered in the analytical method. The calculated stresses are also compared with the resistance of the soil mix material computed considering the design approach of the handbook. Analytical stress values are computed considering: $\alpha_{sm} = \beta = k_f = \gamma_{sm} = 1$ [-] as the characteristic values are used in the numerical simulations.
As a result of the comparison, the numerical values of the stresses obtained with a $f_{sm,tk}$ value of 0.4 MPa are smaller than the analytical values.
With $f_{sm,tk} = 0$ MPa, a relatively good correspondence is observed between the numerical and the analytical results for the maximal shear stress in the pressure arch. The value of the maximal compressive stress at the base of the arch, which is a little bit higher than the analytical value, is obviously dependent on the value of the angle α considered for the pressure arch. A larger difference is still observed for the maximal compressive stress in the middle of the pressure arch. This difference could be explained by the shape of the wall made of secant soil-cement columns resulting in a nonparabolic pressure arch (see Fig. 7). A study is currently conducted to investigate this "shape" effect and to adapt the analytical method of the handbook.

Table 3. FEM and analytical results for the stresses developing inside the pressure arch generated by the application of a uniform pressure of 50 kPa on the wall

	FEM results with $f_{sm,tk}$ = 0.4 MPa [kPa]	**FEM results with $f_{sm,tk}$ = 0 MPa [kPa]**	**Handbook - analytical results [kPa]**	**Handbook - resistance [kPa]**
Maximal† compressive stress at the base of the pressure arch, $\sigma'_{arch,base}$ (kPa)	between 119 and 127 if α is slightly varied‡	between 225 and 262 if α is slightly varied‡	201 See equation [10]	3346
Maximal† compressive stress in the middle of the pressure arch, $\sigma'_{arch;mid;max}$ (kPa)	46 (see Fig. 9 for the selected cross-section)	94 (see Fig. 9 for the selected cross-section)	198 See equation [15]	2362
Maximal† shear stress in the pressure arch, τ_{Ed} (kPa)	59♣ and 66‖	115♣ and 114‖	115 See equation [13]	544

†Maximal stress value for the stress distribution developing along the determined cross-section
‡for the determination of $\sigma'_{arch,base}$, the angle α deduced from the analytical approach is initially used. Afterwards, an extra analysis is conducted varying the value of α to observe the effect of this variation on the value of $\sigma'_{arch,base}$: see Fig. 8 for the cross-section
‖along a cross-section corresponding to the bend in the strut and tie model, i.e. at $l_s/4$: see Fig. 10 for the selected cross-section
♣ along a cross-section at the boundaries of the flanges of the steel beam

ACKNOWLEDGMENTS

This work was supported by the CWALity DE research program of the Walloon Region (Direction des Programmes de Recherche). This support is gratefully acknowledged.

REFERENCES

BBRI/SBRCURnet. 2018. Handbook Soil mix walls. Taylor and Francis Group, ISBN 978 90 5367 641 7.

EN 1992-1-1: 2004. Eurocode 2: Design of concrete structures.